Optimizing Image Segmentation by Chaotic Dynamics

Mikio Hasegawa*[A], Tohru Ikeguchi*, Takeshi Matozaki* and Kazuyuki Aihara**

* Science University of Tokyo, Chiba, 278 Japan, [A]hasegawa@mtlb.te.noda.sut.ac.jp
** University of Tokyo, Tokyo, 113 Japan, aihara@sat.t.u-tokyo.ac.jp

Abstract

We combine an image segmentation method into small regions with chaotic neurodynamics, which has already been clarified to be effective for solving combinatorial optimization problems, in order to improve performance of segmentation. The results with our novel method are compared with the conventional stochastic dynamics for escaping from local minima. As a result, we obtain better results with chaotic neurodynamical image segmentation.

I. Introduction.

In image processing, it is very important to develop an effective algorithm for image segmentation. From the viewpoint of image analysis, it is strongly desirable to segment image into small regions in which all pixels have uniform characteristics. Recently, two novel ideas, the variable-shape-block method (VSB) [1] and the segmentation method using the Voronoi diagrams [2], were proposed to segment image signals into small regions from the viewpoint of image compression. When these methods are applied to high quality image signals, they are very effective and therefore lead to very high compression rates. However, these algorithms have a kind of steepest descent down hill dynamics, namely, in some image signals there are undesirable local minima at which these algorithms get stuck depending on shapes or textures of objects. Furthermore, if image signals are contaminated by noise, it is very hard to find "optimal" shapes of small regions, because the number of local minima may be increased. In order to treat such difficulty, Matsuda et al. applied simulated annealing to the segmentation method by the Voronoi diagrams for improving coding performance [3].

From the viewpoint of solving combinatorial optimization problems, an application of chaotic dynamics has been proposed [4]– [9], and its effectiveness has been shown on the traveling salesman problems (TSP). Therefore it is natural to expect that chaotic dynamics would also be effective for image segmentation. In optimization using chaotic dynamics, there are two approaches; the first one adopts memoryless chaotic sequence ("chaotic noise") [9], and the second one implements chaos into neural networks [10, 11]. The latter has chaotic neurodynamics and memory effect appeared in refractoriness of each neuron [4]–[8].

In this paper, in order to evaluate the effectiveness of chaotic noise, first we investigate what kind of statistics of chaotic noise is effective. Namely we compare the original time series and its surrogate data [12], which is a realization of a stochastic process preserving several statistics, for instance, empirical histograms and autocorrelation. Then, we apply chaotic neurodynamics to the VSB [1] for optimizing block shapes and compare performance on segmentation by chaotic dynamics with stochastic dynamics.

II. The algorithm of the variable-shape-block method [1].

The basic algorithm introduced in this paper, the VSB, is shown in Fig.1. First, an original image signal is divided into small squares (an initial state). Then, a criterion for evaluating a state of segmentation is introduced; this is called an evaluation parameter and is a kind of energy [1, 2, 3]. For evaluating a position of each vertex P on quadrangles shown in Fig.1, an evaluation parameter E_P on the position is defined as follow,

$$E_P = \sum_{l \in R} S_l \qquad (1)$$

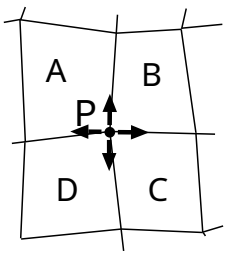

$E_P = S_A + S_B + S_C + S_D$
S_l:error of the region l

$(l = A, B, C, D)$

Figure 1: Schematic representation of a movement of a vertex P and its regions A,B,C and D.

where S_l is a feature of the region l, and R is the set of the regions which belong to the vertex P. In this paper, $S_l = \sum_{ij \in l} |G_{ij} - \bar{G}_l|$, where G_{ij} is a gray level of the ij th pixel, and $\bar{G}_l$ is mean of gray levels of pixels belonging to the region l. Since the shape of small regions is a quadrangle, the number of R is four (in Fig.1, $R = \{A, B, C, D\}$). Next, by moving the vertex P to the four directions, namely, upward, downward, leftside and rightside, the evaluation parameters E_{P_i} at each direction $i (i = 1 \sim 4)$ are calculated. Then vertex P is moved to the i th direction corresponding to the smallest evaluation parameter. Repeating this procedure for all vertices on quadrangles, we obtain the image signals segmented into small regions which have a uniform feature [1].

Since the procedure has a kind of steepest descent down hill dynamics, there are many undesirable local minima depending on their shapes and noise in image signals. Then it is considered to be effective to make a state of vertices escape from those local minima by chaotic dynamics.

III. Chaotic dynamics for optimization.

A. *Estimation of effectiveness of chaotic noise using the method of surrogate data [12].*

In this subsection, we estimate the effectiveness of chaotic noise for solving combinatorial optimization problems. Applying Hopfield neural network to the TSP [13], we estimate the effectiveness of adding chaotic noise by comparing surrogate data sets [12, 9]. In this paper, three algorithms for making surrogate data are introduced. The first surrogate data is made by random shuffling of the original data. The second surrogate data is made by the following procedure: first, the Fourier transform of the original data is calculated to obtain a power spectrum. Then phases of the power spectrum is randomized, finally the inverse Fourier transform is calculated. The obtained surrogate data has an identical power spectrum with the original data, then it is called phase-randomized surrogate. The third surrogate is made by almost the same procedure as the second one. It preserves exactly an empirical histogram and is called Gaussian-scaled surrogate.

In Fig. 2, the autocorrelation function of logistic map, $z(t+1) = rz(t)(1 - z(t))$, and those of surrogates are shown in case of $r = 3.95$. It is clearly seen that autocorrelation function of the second surrogate is exactly the same as the original and that autocorrelation of the third surrogate is almost the same. The first surrogate data has quite different autocorrelation from the original. The results of solving combinatorial optimization problems using a logistic map and its surrogates are shown in Fig.3 in case of changing r. From this result, the first surrogates have quite different solving abilities from ones of the original data, and

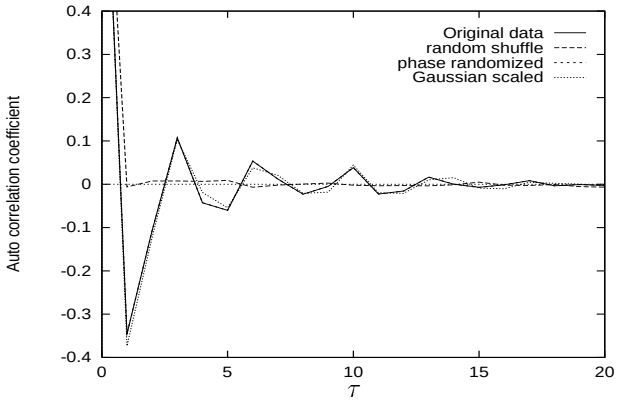

Figure 2: Autocorrelation function of a logistic map and its surrogate data. The number of time series is 16384.

the second and third surrogates have similar abilities to the original data. It means that the temporal structure of chaotic noise characterized by autocorrelation affects for solving optimization problems. High solving abilities of phase randomized and Gaussian scaled surrogates on the range of $3.86 < r < 4.0$ suggests that there is no need to use chaotic noise for solving optimization problems. The results of optimization of the VSB by adding logistic maps are shown in Table 1 (a). It is clearly seen that using chaotic noise have better solutions than Gaussian random numbers.

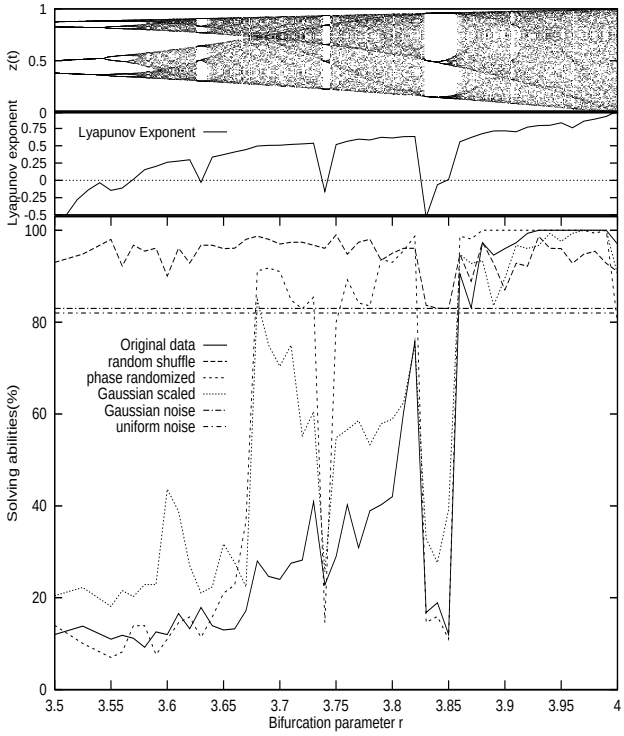

Figure 3: Solving abilities of a 10-city TSP with a logistic map and its surrogates. The upper figure shows the bifurcation diagram of a logistic map, and the middle shows Lyapunov exponents in case of changing parameter r.

B. Optimization and Chaotic neurodynamics.

Then, we considered to use chaotic neurodynamics, which have a memory effect in refractoriness. On optimization, it is important to retrieve directions which have already searched. Our previous results showed that weak chaos has higher solving abilities [8]. Further, the effectiveness of chaotic neurodynamics was suggested by comparing with a random neuron model which has no memory [5]. In this paper, we use chaotic neurodynamics for optimization [10, 11]. The dynamics of the i th chaotic neuron in a chaotic neural network is defined as follow:

$$\begin{aligned} x_i(t+1) = f_i[&\sum_{j=1}^{N_A} V_{ij} \sum_{d=0}^{t} k_s^d A_j(t-d) \\ &+ \sum_{j=1}^{N_x} W_{ij} \sum_{d=0}^{t} k_m^d x_j(t-d) \\ &- \alpha \sum_{d=0}^{t} k_r^d x_i(t-d) - \theta_i], \end{aligned} \tag{2}$$

where $x_i(t+1)$ is the output of the i th chaotic neuron at discrete time $t+1$; $A_j(t)$ is the strength of the jth externally applied input at the discrete time t and N_A is the number of the externally applied inputs; V_{ij} is the connection weight from the jth externally applied input to the i th chaotic neuron; W_{ij} is the connection weight from the j th chaotic neuron to the i th chaotic neuron; f_i is the continuous output function of the i th chaotic neuron; a_i is the threshold of the i th chaotic neuron; k_s,k_m and k_r are the decay parameter for external inputs, feedback inputs and refractoriness, respectively[10].

Defining three internal states corresponding to externally applied inputs, mutual interactions and refractoriness by ξ_i, η_i and ζ_i, then, we obtain a reduced form of chaotic neural networks shown in the following equations:

$$\xi_i(t+1) = k_s \xi i(t) + \sum_{j=1}^{N_A} V_{ij} A_j(t), \tag{3}$$

$$\eta_i(t+1) = k_m \eta_i(t) + \sum_{j=1}^{N_x} W_{ij} x_j(t), \tag{4}$$

$$\zeta_i(t+1) = k_r \zeta_i(t) - \alpha x_i(t) + a_i, \tag{5}$$

$$x_i(t+1) = f_i[\xi_i(t+1) + \eta_i(t+1) + \zeta_i(t+1)], \tag{6}$$

where f_i is a sigmoidal function, $f_i(z) = 1/(1 + \exp(-z/\epsilon))$ and $a_i = -\theta_i(1-k_r)$.

IV. Image Segmentation using Chaotic Neurodynamics.

The algorithms that have been adopted for solving combinatorial optimization problems by neural dynamics need mutual connections which has the information to minimize the energy function. However, it is not only difficult but also impossible to construct such objective function of neural networks for the VSB in a real situation because each state in the VSB must be expressed only by 0 and 1 in such neural networks. So we made a very simple type of neural network model suitable for the VSB.

The new rule for moving vertices is defined as follows. Let each neuron have four internal states $\xi_{P_i}(t)$ $(i = 1, \ldots, 4)$ corresponding to four directions and one internal state $\zeta_P(t)$ to the refractoriness. The dynamics of moving vertices is defined as follows:

$$\xi_{P_i}(t+1) = k_s \xi_{P_i}(t) + h(E_0 - E_i), \tag{7}$$

$$\zeta_P(t+1) = k_r \zeta_P(t) - \alpha[\sum_{j=1}^{4} M_{P_j}(t)] + a_P, \tag{8}$$

$$M_{P_i}(t+1) = f[\xi_{P_i}(t+1) + \zeta_P(t+1)], \tag{9}$$

where $E_i (i = 1 \ldots 4)$ is the evaluation parameter in case of moving to the i th direction. E_0 is calculated for the vertex P at the present position. If an M_{P_i} is larger than a threshold θ and the largest in all i, it can be considered that the neuron corresponding to the i th direction fires, then the vertex P moves to the direction i. With this rule, each vertex can not stay in the same position, therefore vertices can escape from undesirable local minima.

V. Results.

The results with and without chaotic neurodynamics are shown in Fig. 4. The size of the original image is 256×256 pixels. In Fig. 4, the sum of absolute values of the difference from the mean of gray levels is used as an error S_l in Eq. (1), and an initial state is 8×8 blocks. The result using chaotic neurodynamics is solved with $k_r = 0.9, k_s = 0.0, \alpha = 0.25, a_P = 0.35, \epsilon = 0.02, \theta = 0.5, f(z) = 1/(1 + \exp(z/\epsilon))$. Further we introduced a chaotic neurodynamical simulated annealing which is realized with normalizing function (Eq. (7)) $h(z) = z/(256 \times b \times T)$, where 256 is a total gray level, b is a normalization parameter, and T is the temperature parameter for simulated annealing. The result in Fig. 4 is obtained with $b = 0.005, T = 0.985^t$. It is seen that the result using chaotic dynamics is qualitatively better than the conventional one, for example, around eyes or the mouth of a woman.

Then, the results of chaotic neurodynamical segmentation are compared with the results of the VSB with adding stochastic dynamics. In order to implement the VSB with random dynamics, Gaussian distributed random numbers are added to each evaluation parameter on each state. In a similar way, stochastic simulated annealing is also introduced by reducing variance of random numbers with cooling parameter C_o. Tables 1 (b) and (c) show the average solutions of the VSB with stochastic dynamics and chaotic neurodynamics, $k_m = 0.0, \alpha = 0.25, \epsilon = 0.2, a_P = 0.35$ for all $P, b = 0.003$, respectively. Tables 1 (d) and (e) are stochastic simulated annealings with changing

Figure 4: The original image (left), the result by conventional variable-shape-block method (center) and chaotic neurodynamical simulated annealing (right).

Table 1: Average solutions of the VSB with (a) chaotic noise (the logistic map) on changing variance, (b) random numbers on changing variance, (c) chaotic neurodynamics on changing k_r, (d) stochastic simulated annealing on changing cooling parameter C_o, and (e) chaotic neurodynamical simulated annealings on changing k_r.

(a)

Variance	0.3	0.4	0.5	0.6	0.7
Results($\times 10^6$)	7.20	7.05	7.06	7.17	7.26

(b)

Variance	0.3	0.4	0.5	0.6	0.7
Results($\times 10^6$)	7.13	7.06	7.06	7.09	7.11

(c)

k_r	0.5	0.6	0.7	0.8	0.9
Results($\times 10^6$)	7.42	7.18	7.07	6.94	6.90

(d)

C_o	0.95	0.975	0.985	0.995
Results($\times 10^6$)	7.42	7.08	6.84	6.78

(e)

k_r	0.5	0.6	0.7	0.8	0.9
Results($\times 10^6$)	6.89	6.80	6.73	6.70	6.70

cooling parameters, and chaotic neurodynamical simulated annealings, $k_m = 0.0, \alpha = 0.25, \epsilon = 0.2, a_P = 0.35$for all $P, b = 0.008, t = 0.985$ in case of changing k_r. These results are average values of total absolute errors with 10 diffrent initial conditions.

Fig.5 shows temporal changes of the total evaluation parameter E for all vertices in case of introducing chaotic neurodynamics and random dynamics. In Fig. 5 shown are the best results of each methods. From these results, it is clarified that the result using chaotic dynamics has better solving ability than stochastic dynamics and that chaotic simulated annealing has the best performance.

VI. Conclusions.

In this research, we have applied chaotic neurodynamics to image segmentation. We used chaotic neural networks for finding "optimal" position of vertices of the VSB. Our model produces not only chaotic dynamics, but also has memories by refractory effects, our method exhibits good performance. It is very effective and important to consider the direction which have already searched in case of moving

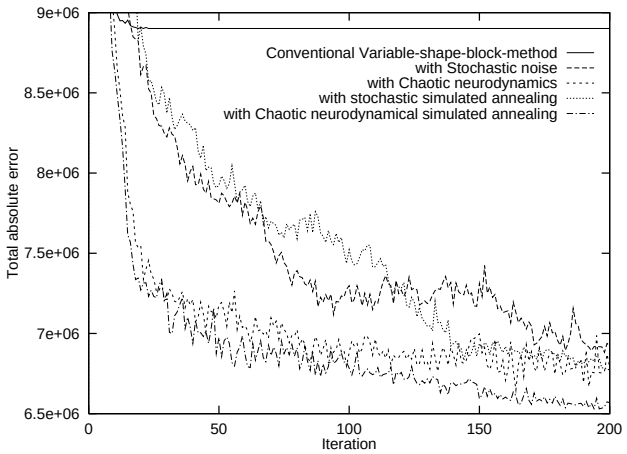

Figure 5: The total evaluation parameter E.

vertices. It is an important future problem to apply this model to other problems, and investigate what is the effectiveness of chaotic dynamics for combinatorial optimization problems and what kind of chaos is suitable to those problems [14]. The authors would like to thank I.Matsuda(Science University of Tokyo) and T.Yamada(Aihara Electrical Engineering Co.,Ltd.) for their fruitful discussions.

References

[1] I.Matsuda et al.: The journal of ITM, 47, 10, 1277, 1993.
[2] I.Matsuda et al.:ITE Technical Report, IE 95-16, 1994.
[3] I.Matsuda et al.: IEICE spring conference, D-299, 1995.
[4] H.Nozawa: Chaos, 2, 3, pp. 377-386, 1992.
[5] T.Yamada et al.: Proc. of IEICE NOLTA, Vol. 4, 10.3-6, 1173, 1993.
[6] T.Yamada et al.: Proc. of IEEE ETFA, 1994.
[7] L.Chen et al.: Proc. of IEICE NOLTA, Vol. 2, 5.7-5, 695, 1993.
[8] M.Hasegawa et al. :Proc. of IEEE ICNN '95, Perth, 1995.
[9] Y.Hayakawa and Y.Sawada: Technical Report of IEICE, NLP 94-39, 1994.
[10] K.Aihara, et al.: Phys. Lett. A, 144, 333, 1990.
[11] K.Aihara: in "Bifurcation Phenomena in Nonlinear Systems and Theory of Dynamical Systems," ed. H.Kawakami, 143, World Scientific, 1990.
[12] J.Theiler et al.:Physica D 58, pp. 77-94, 1992.
[13] J.J.Hopfield and D.W.Tank: Biol. Cybern. 52, 144, 1985.
[14] M.Hasegawa et al.:in preparation.